Requirements for T Lymphocyte Migration in Explanted Lymph Nodes[1]

Julie H. Huang,* L. Isabel Cárdenas-Navia,† Charles C. Caldwell,‡ Troy J. Plumb,§ Caius G. Radu,¶ Paulo N. Rocha,‖ Tuere Wilder,# Jonathan S. Bromberg, Bruce N. Cronstein,# Michail Sitkovsky,†† Mark W. Dewhirst,†‡‡ and Michael L. Dustin[2]***

Although the requirements for T lymphocyte homing to lymph nodes (LNs) are well studied, much less is known about the requirements for T lymphocyte locomotion within LNs. Imaging of murine T lymphocyte migration in explanted LNs using two-photon laser-scanning fluorescence microscopy provides an opportunity to systematically study these requirements. We have developed a closed system for imaging an intact LN with controlled temperature, oxygenation, and perfusion rate. Naive T lymphocyte locomotion in the deep paracortex of the LN required a perfusion rate of >13 μm/s and a partial pressure of O_2 (pO_2) of >7.4%. Naive T lymphocyte locomotion in the subcapsular region was 38% slower and had higher turning angles and arrest coefficients than naive T lymphocytes in the deep paracortex. T lymphocyte activation decreased the requirement for pO_2, but also decreased the speed of locomotion in the deep paracortex. Although CCR7$^{-/-}$ naive T cells displayed a small reduction in locomotion, systemic treatment with pertussis toxin reduced naive T lymphocyte speed by 59%, indicating a contribution of Gα_i-mediated signaling, but involvement of other G protein-coupled receptors besides CCR7. Receptor knockouts or pharmacological inhibition in the adenosine, PG/lipoxygenase, lysophosphatidylcholine, and sphingosine-1-phosphate pathways did not individually alter naive T cell migration. These data implicate pO_2, tissue architecture, and G-protein coupled receptor signaling in regulation of naive T lymphocyte migration in explanted LNs. ***The Journal of Immunology,*** **2007, 178: 7747–7755.**

The adaptive immune response requires matching the Ag TCR repertoire to peptide-MHC adducts that can enter the body at any location to sense pathogens that enter the body at any location (1, 2). Because each TCR specificity is borne on a few hundred T cells, the problem of bringing these T cells to the dendritic cells (DC)[3] (3) bearing the pathogen-derived peptide-MHC is formidable (3). The first step is for DC to gather Ags from the tissues or blood (4, 5). In the second step, the DC migrate to the lymph nodes (LNs) and form networks in the T cell zones of LNs and/or the spleen (6–8). Then, T cells enter the LN or spleen from the blood and survey the DC networks to detect Ags (9–11). Insights into the nature of the final step in which T cells scan DC networks for Ag have been provided by two-photon laser-scanning microscopy, which allows microscopic examination of fluorescent T cells and DC interacting in live tissues or animals (12–14).

The first insights into this repertoire-scanning process were obtained by imaging T cell movement in explanted LNs. In these experiments, fluorescent T cells were transferred into nonfluorescent recipient mice and allowed to enter LNs via the high endothelial venules; the LN was removed without disrupting the capsule and perfused with 95% O_2 equilibrated medium (partial pressure of O_2 (pO_2) = 95%). Under these conditions, T cells were observed to migrate rapidly and randomly with an average velocity of 10.8 μm/min and a motility coefficient for the three-dimensional (3D) random walk of 67 μm^2/min (13). Similar results were obtained in vivo suggesting that the high pO_2 was compatible with physiological migration patterns (15). Recent studies suggest that T cells navigate in the LN by crawling along stromal cell networks that underlay the DC networks and are even more elaborate than previously anticipated (16). Nonetheless, the pattern of in vivo migration can be described as autonomous in that the T cells appear to turn in random fashion as long as they remain in the T cell zones. Although T cell direction appears to be chosen at random in the 3D lattice, the signaling processes that motivate the T cells are not known.

Imaging lymphocyte migration in explanted LNs provides an opportunity to study the molecular and physical requirements in a way that would be difficult or impossible in a live mouse. T lymphocytes in the periphery face a wide range of pO_2 from as high as

*Program in Molecular Pathogenesis, Kimmel Center for Biology and Medicine, Skirball Institute, New York University School of Medicine, New York, NY 10016; †Department of Biomedical Engineering, Pratt School of Engineering, Duke University, Durham, NC 27708; ‡Laboratory of Trauma, Sepsis and Inflammation Research, Department of Surgery, University of Cincinnati, Cincinnati, OH 45267; §Department of Internal Medicine, Section of Nephrology, University of Nebraska Medical Center, Omaha, NE 68198; ¶Department of Microbiology, Immunology and Molecular Genetics, University of California, Los Angeles, CA 90095; ‖Division of Nephrology, Duke University, Durham Veterans Affairs Medical Centers, Durham, NC 27705; #Divisions of Clinical Pharmacology and Rheumatology, Department of Medicine, New York University School of Medicine, New York, NY 10016; **Department of Gene and Cell Medicine, Mount Sinai School of Medicine, New York, NY 10029; ††Departments of Biology and Pharmaceutical Sciences, Northeastern University, Boston, MA 02115; and ‡‡Department of Radiation Oncology, Duke University Medical Center, Duke University, Durham, NC 27710

Received for publication February 12, 2007. Accepted for publication April 4, 2007.

The costs of publication of this article were defrayed in part by the payment of page charges. This article must therefore be hereby marked *advertisement* in accordance with 18 U.S.C. Section 1734 solely to indicate this fact.

[1] This work was supported by National Institutes of Health Grants AI55037 (to M.L.D.) and DK38108 (to T.J.P. and P.N.R.) and the Irene Diamond Foundation (to M.L.D.).

[2] Address correspondence and reprint requests to Dr. Michael L. Dustin, Program in Molecular Pathogenesis, Skirball Institute, New York University Medical Center, 540 First Avenue, New York, NY 10016. E-mail address: dustin@saturn.med.nyu.edu

[3] Abbreviations used in this paper: DC, dendritic cell; LN, lymph node; pO_2, partial pressure of O_2; 3D, three dimensional; PTX, pertussis toxin; WT, wild type; GPCR, G protein-coupled receptor; TP, thromboxane-prostanoid receptor; ETYA, 5,8,11,14-eicosatetraynoic acid; 2D, two dimensional; $A_{2A}R$, A_{2A} adenosine receptor; S1P, shpingosine-1-phospate.

20% in lung alveoli to 1–5% in most peripheral tissues including secondary lymphoid tissues and <1% in sites of tissue injury or necrosis (17). Perfusion and high pO_2 are the most commonly used in vitro conditions, but quantitative studies on requirements for either of these parameters have not been performed. Because secondary lymphoid organs are thought to be typical of most tissues with pO_2 in the range of 1–5% (17), it is unclear whether the high extranodal pO_2 conditions are required to achieve a physiological pO_2 within the LN due to the diffusion barrier of the capsule and the depth of the T cell zones or whether the pO_2 in the T cell zones is superphysiological under these conditions (15, 18).

In this study, we investigated the role of O_2 and perfusion as chemokinetic factors for T cell migration in explanted LNs and compared the role of O_2 to that of signaling through $G\alpha_i$-coupled receptors classically linked to cell migration. We have also investigated the role of a number of specific G protein-coupled receptors (GPCR) to determine whether these candidates have a nonredundant role in regulating T cell migration. We focused on one chemokine receptor, CCR7, as an important candidate upstream of $G\alpha_i$ (19–21). We found that perfusion above a threshold velocity with pO_2 levels ~2-fold higher than physiological measurements is critical for migration of naive T cells in explanted LN. Activated T cells migrate more slowly, but with a low pO_2 threshold. Surprisingly, no single upstream receptor could be identified as important in T cell migration in the explanted LNs, but elimination of all $G\alpha_i$-mediated signaling profoundly decrease T cell migration.

Materials and Methods

Mice

DO11.10 on the B10.D2 background (>10 generated backcrossed) and B10.D2 mice ranging from 6 to 12 wk of age were used in all experiments, except $CCR7^{-/-}$ mice (19) were on the B6 or BALB/c background and $A_{2A}R^{-/-}$ mice (22) were on the B6 background. All mice were bred and maintained in accordance with the Institutional Animal Care and Use Committee guideline of New York University School of Medicine. BALB/c mice for the CCR7 experiments were purchased from The Jackson Laboratory.

Cells

Naive DO11.10 T lymphocytes were purified by negative selection using magnetic beads from the pan-T selection kit (Miltenyi Biotec). The cells were then labeled with 1 μM CFSE at room temperature for 15 min in 2 mM HEPES, 13.8 mM NaCl, 0.5 mM KCl, 0.07 mM Na_2HPO_4, and 0.6 mMD-glucose (HBS). The concentration of dye was chosen through systematic preliminary studies balancing fluorescence intensity, viability, and chemotactic responses in vitro. It was important to include 5 mM D-glucose during labeling. A total of 5–10 million labeled cells were adoptively transferred via tail vein injection to the host B10.D2 mice 1 day before imaging. By flow cytometry, we found the injection of 3×10^6 cells results in 0.3–0.5% CFSE-positive cells in the inguinal LN at day 3.

For blast preparation, we mixed 350 μg of OVA peptide and 5 μg of LPS for tail vein injection along with the CFSE-labeled naive cells. Imaging was performed 24 h after transfer and initiation of activation. The activation status was confirmed via FACS analysis.

Where indicated, mice were injected with 200 μg/kg pertussis toxin (PTX) (Calbiochem) or the same volume of PBS 12–16 h after adoptively transferring naive T lymphocytes. Imaging of explanted LNs was performed at 18–24 h after the treatment.

Measurement of LN pO_2

pO_2 was measured with a recessed-tip O_2 microelectrode having a tip diameter of 9–12 μm (23). Depth of insertion in the LN was controlled with a micromanipulator. Electrode current was measured with a minisensor and recorded by a computer. For intravital measurements, the inguinal LN was exposed and immobilized to allow electrode insertion. For ex vivo analysis, the mouse was sacrificed and the inguinal LN was removed. After measuring the size of the LN, ethyl cyanoacrylate adhesive (Elmer's Products) was used to fix the LN on nylon mesh in a petri dish, the LN was then submerged in Invitrogen Life Technologies Leibovitz's L-15 medium equilibrated with a range of O_2:N_2 gas mixtures.

The measurement of each LN started from the capsule and the probe was inserted at increments of 50 μm. Measurements of pO_2 inside the LN were taken at 10 different locations and angles to a maximal depth approximately half the diameter of the LN and pO_2 vs depth was plotted. All measurements were obtained at 35–37°C.

Explanted LN imaging and pO_2 measurement

The setup was composed of a heated flow cell (Bioptechs) with a flow channel 1 mm high and 1.3 mm wide and a syringe pump (Harvard Apparatus) to provide a regulated perfusion velocity. The perfusion velocity was defined as the flow rate (volume/time) divided by the cross-sectional area of the flow channel (area) to yield a linear average velocity (distance/time). We neglected local changes in velocity that would be expected due to the parabolic flow in the parallel plate flow cells and the disturbance of flow by the LN itself, which covers <10% of the area of the flow channel. O_2:N_2 mixes were bubbled with a gas dispersion tube into the medium reservoir to provide regulated pO_2. A special adapter was purchased from Bioptechs to allow the mounting of the flow cell, which is typically used on an inverted microscope, for use on an upright microscope. The O_2 level in the system is measured with a fiber optic O_2 probe that measures luminescence lifetime and does not consume O_2 during the measurement (Oxymicro; WPI), which allowed for accurate, constant monitoring of pO_2. The fiber optic probe was placed at the outlet of the flow cell such that medium pO_2 was read throughout the experiment 300 μl downstream of the Bioptechs flow cell containing the LN.

Two-photon microscopy

We used a custom-built system for our two-photon imaging (24, 25). It consists of a modified upright Olympus microscope and a modified confocal scan head fitted with a ×60 water immersion objective (NA = 0.9) and a Spectra-Physics Tsunami femtosecond laser tuned to 780 nm (26). A nondescanned photomultiplier tube mounted off the epifluorescence filter turret was used to detect fluorescence emission of <700 nm (12). Data acquisition were controlled by the Fluorview software and analyzed using Volocity (Improvision). T lymphocyte position over time was determined by acquiring XYZ stacks of 10–25 XY images of 512 × 512 pixels (236 × 236 μm) with an axial spacing of 2–3 μm. These XYZ stacks were acquired every 30 s for 15–30 min; X, Y, Z, T data sets were then used to calculate the instantaneous velocity, turning angle, confinement index, and arrest coefficient. The instantaneous velocity of fixed points in the tissue was not >1.5 μm/min when determined by tracking with Volocity. Thus, 1.5 μm/min was used as a threshold for immobility when calculating the arrest coefficient.

Statistics

Comparisons were analyzed for statistical significance using KaleidaGraph 4.0 software (Synergy). Nonparametric methods such as Wilcoxon-Mann-Whitney test or ANOVA were used to determine significance.

Results

Intravital measurement of pO_2 in LNs

To have a point of reference for ex vivo studies, we first determined the pO_2 in the inguinal LN in vivo using an O_2 microelectrode. This approach has been extensively used in tumor and muscle tissues (27). The probe was calibrated using buffer solutions saturated with different gas mixes. The inguinal LN was exposed and immobilized using the same surgical approach as used for intravital imaging (28). The physiological pO_2 in the LN was between 0.5 and 6% and varied by location or depth (Fig. 1). The overall mean value for all measurements was 2.2%. The sudden increase of pO_2 in some traces may be due to the probe encountering capillaries. Similar results were obtained from a previous study focusing on normal spleen (17) and muscle (27).

Measurement of pO_2 in explanted LNs

To determine how pO_2 within an explanted LN relates to the pO_2 in the perfusing medium, we performed O_2 microelectrode experiments on excised LNs. We perfused the excised LN in a 37°C bath that was vigorously bubbled with different O_2:N_2 gas mixes. The

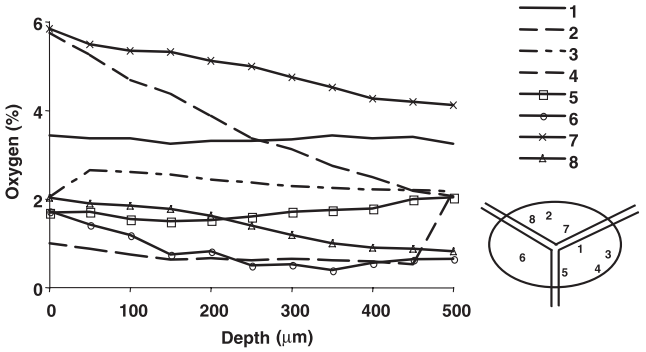

FIGURE 1. Direct pO_2 measurements in LN in vivo. Each line represents measurements alone one track from the point of microelectrode probe insertion up to 500 μm deep into the LN at 50-μm steps. Each point of measurements is an average of pO_2 readout over 10–30 s. Each track was measured from a different location on the LN and the track location was represented on the inguinal LN schematic at the *lower right* side. The experiment shown is representative of four LNs.

bubbling both saturated the medium at a particular pO_2 and provided turbulent mixing around the LN to ensure that the medium was moving rapidly over the surface of the LN. Then, we measured the change of pO_2 within the LN at different depths using the microelectrode (Fig. 2*A*). Surprisingly, pO_2 was independent of depth up to 500 μm. Media and LN pO_2 were linearly correlated (Fig. 2*B*). We conclude that O_2 penetrates rapidly into the LN and that O_2 consumption in the tissues did not substantially reduce the pO_2 during this diffusion/transport process. Thus, it was not necessary to use high-medium pO_2 to obtain physiological pO_2 at up to 500 μm.

Effect of perfusion velocity on naive T lymphocyte locomotion

Bousso and Robey (29) noted that moving perfusion is essential for naive T lymphocyte movement, but did not quantify the requirement. We determined the effect of flow velocity on the migration speed of naive T lymphocytes measured by two-photon time-lapse microscopy at 150-μm depth in the deep paracortex. Naive T lymphocytes moved rapidly when the flow velocity was set at 40 μm/s or faster at 20% pO_2, and were immobile (speed lower than 1.5 μm/min) at flow velocities of 13 μm/s or less, regardless of pO_2 (20–100%) (Fig. 3). It should be noted that extranodal pO_2 was maintained at over 15% without perfusion in

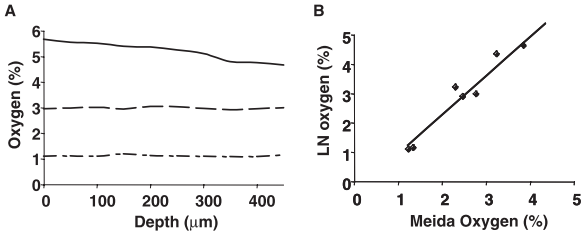

FIGURE 2. Measurements of pO_2 in explanted LN. *A*, Three lines represent three independent measurements of pO_2 at increments of 50 μm into the explanted LN, each in medium equilibrated with different gas mixtures. This provides a readout of environment medium pO_2 shown as 0 μm. The medium (L-15) was vigorously bubbled with O_2:N_2 gas mixes and the explanted LN was glued down on a nylon mesh fixed on a petri dish. The setup was submerged in L-15 while maintaining at 35–37°C throughout the experiment. *B*, The correlations between medium pO_2 and the average LN pO_2 are high (R = 0.95). Each dot represents an average of LN pO_2 measured at a fixed depth and medium pO_2. Representative of five LNs.

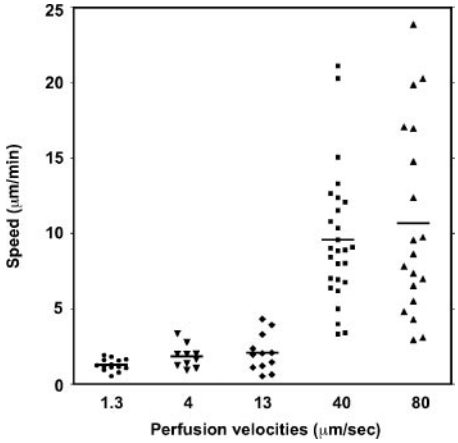

FIGURE 3. Perfusion requirements for naive T lymphocyte locomotion in explanted LNs. Each column represents one flow velocity set by the syringe pump under controlled temperature and pO_2. Each dot represents the average speed of one single cell, which was calculated by dividing the path length over time. The bar in each column represents the average speed of all the cells tracked. The medium was equilibrated at 20% pO_2. Tracks from two LNs are shown.

our system, which was sufficient for naive T lymphocyte migration when perfusion was set at 40 μm/s (see below). Whether this requirement was due to decreased pO_2 in the LN or due to some

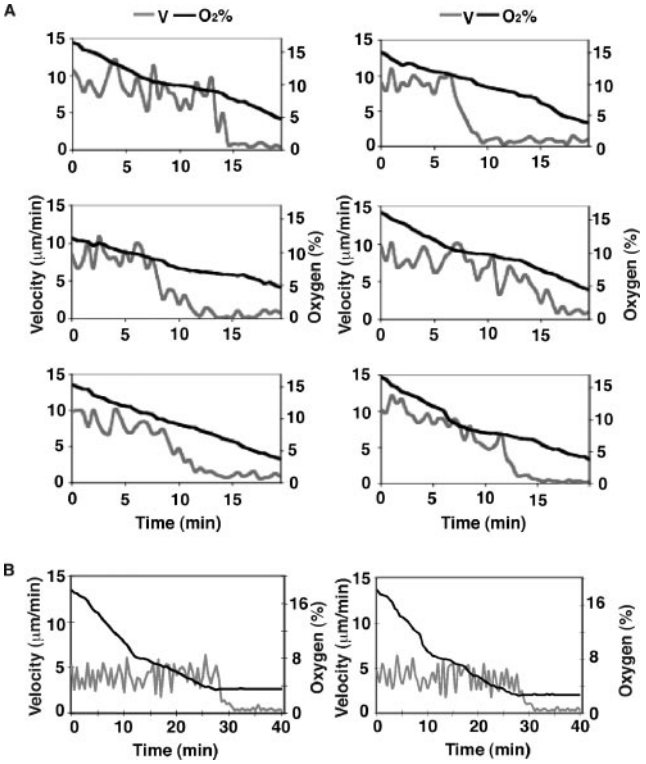

FIGURE 4. O_2 requirements for naive and activated T lymphocyte locomotion. *A*, The real-time measurement of naive T lymphocyte locomotion vs environmental pO_2. Each graph represents one data set and the black line demonstrates the drop of pO_2 that was recorded by Oxymicro while constantly purging O_2 in the system. The gray line is the average instantaneous velocity of at least three cells in the filed of image and the *x*-axis represents time. *B*, Activated T lymphocyte requires less O_2 to maintain locomotion. Using same type of measurement, the two graphs show that in these two data sets, the activated T lymphocytes maintaining locomotion until pO_2 drops to 3–4%. Each panel is a single experiment. A total of three experiments were performed for naive and activated T lymphocytes to obtain average values for thresholds.

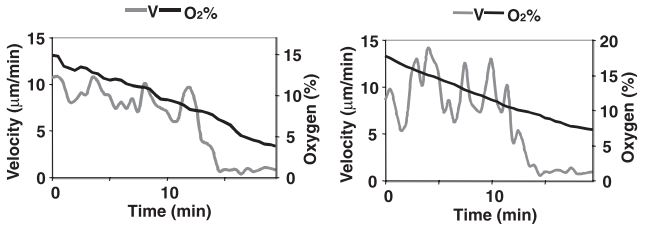

FIGURE 5. $A_{2A}R^{-/-}$ T lymphocytes stopped migrating at the same pO_2 as control cells. The real-time measurement of control (*left*) and $A_{2A}R^{-/-}$ (*right*) T cell locomotion vs environmental pO_2. Each graph represents one data set and the black line demonstrates the drop of pO_2 that was recorded by Oxymicro while constantly purging O_2 in the system. Gray line is the average instantaneous velocity of at least three cells in the filed of image and the *x*-axis represents time.

other effect of perfusion, such as delivering a nutrient or removing a waste product, was not determined.

Effect of pO_2 on naive T lymphocyte locomotion

We performed real-time pO_2 titrations. We started imaging CFSE-labeled T lymphocytes in the LN perfused at 20% pO_2 with a flow velocity of 40 μm/s and then slowly purged O_2 from the medium in the reservoir by bubbling with 100% N_2, while imaging the LN. This resulted in a decrease in pO_2 of ~0.5%/min, which was directly measured with an inline pO_2 sensor and plotted against the instantaneous speed of CFSE-labeled naive T lymphocytes in the 3D imaging volume (Fig. 4*A*). Cell movement stopped at an average of 7.4 ± 1.7% pO_2 and was at 50% maximal speed at 10.4 ± 1.2% pO_2. The pO_2 required to support T lymphocyte locomotion in the perfused explanted LNs was greater than the physiological pO_2 by ~2-fold.

Effect of adenosine receptor $A_{2A}R$

The result from the O_2 experiments led us to investigate whether the sensitivity of lymphocytes to pO_2 reflected a regulatory strategy in vivo. When inflammation or tissue damage-associated hypoxia occurs, it is thought that the hypoxia-induced adenosine accumulation triggers increased cytoplasmic cAMP in immune cells via A_{2A} adenosine receptors ($A_{2A}R$), leading to down-regulation of inflammation (see review in Ref. 30). We hypothesized that this pathway may also modulate T lymphocyte migration at low pO_2 such that antagonism or deficiency of $A_{2A}R$ could result in motility at lower pO_2.

We tested this hypothesis in two ways. We visualized naive T lymphocyte locomotion in LNs isolated from mice transferred with CFSE-labeled wild-type (WT) T cells and treated with ZM241385, an $A_{2A}R$ antagonist, or from WT mice transferred with CFSE-labeled $A_{2A}R^{-/-}$ T cells. Neither of these conditions revealed any changes in pO_2 sensitivity of naive T cell migration (Fig. 5).

T lymphocyte features in different LN areas, activation states, and role of $G\alpha_i$

We next wanted to ask whether there is any difference in the cell motility at different depths within a LN using the two-photon imaging system in shallow and deep regions. We tracked T lymphocyte movements and then calculated the speed, turning angle, confinement index, and arrest coefficient to determine whether naive T lymphocytes had different types of mobility in the shallow and deep compartments within a LN. The turning angle and confinement index quantify the nonlinear nature of T lymphocyte movement. The higher the turning angle the less linear the cell movement. Confinement index is defined here as 1 minus the maximum cell displacement over total path length; therefore, a higher confinement index is representative of greater nonlinearity. The arrest coefficient is the proportion of time that lymphocytes were moving <1.5 μm/min (defined as stopped). We define the shallow region in our system as the subcapsulary sinus, the compartment that is underneath the capsule and surrounding the cortex and we generally collect data from a depth of 20–50 μm below the capsule. We visualized the capsule using the second harmonic signal of the collagen fibers. We define our deep region as the area deeper than 150 μm from the surface, which corresponds to interfollicular to deep paracortex T cell zones. These locations were defined in early articles (31) and immunostaining of LN by us and other researchers (8, 32) is consistent with these definitions.

T lymphocytes moved significantly slower in the shallow compared with deep regions (median velocity 5.68 vs 9.22 μm/min) (Table I). We found that shallow cells were moving with significantly less directionality, as the shallow cells had an median turning angle of 77° while deep cells had an median turning angle of 47°. The confinement indices for the shallow and deep cells were 0.63 and 0.42, respectively ($p = 0.05$), although the shallow cells had a higher arrest coefficient (0.33) compared with deeper cells (0.23), this difference was not statistically significant ($p = 0.14$). Thus, we conclude that T lymphocyte movement was both slower and more confined in the shallow subcapsulary region, but slowing was not attributed to increased cell arrest alone.

To address whether activation states could alter the migration properties of T lymphocytes, we activated the naive DO11.10 T lymphocytes by injecting OVA peptide in vivo and then waited 24 h before imaging migration of the in vivo-activated T lymphocytes. At this time, T lymphocytes are resuming migration after early arrest with APC (14, 18, 33). We determined the level of

Table I. *Summary table of T lymphocyte motility parameters for experiments determining the importance of depth, activation state, CCR7, and G_i PCR*[a]

Experiment	Cell Type	Median Velocity (μm/min)		Arrest Coefficient (%)		Confinement Index (%)		Median Turning Angle (°)	
Depth	Deep	9.22	$p < 0.0001$	22.58 ± 2.2	$p = 0.14$	58.21 ± 3.9	$p = 0.05$	47.39	$p < 0.0001$
	Shallow	5.68		33.18 ± 6.2		37.32 ± 5.0		77.34	
Activation	Naive	9.16	$p < 0.0001$	23.08 ± 4.1	$p = 0.48$	60.38 ± 5.2	$p = 0.07$	60.34	$p < 0.0001$
	Activated	4.16		31.68 ± 15.3		46.26 ± 2.5		49.95	
Gα-i	Control	10.45	$p < 0.0001$	18.64 ± 0.3	$p = 0.04$	60.25 ± 5.6	$p = 0.01$	46.49	$p < 0.0001$
	PTX treated	4.1		53.96 ± 13.1		43.83 ± 5.3		84.2	
CCR7	Control	11.2	$p = 0.06$	17.96 ± 1.1	$p = 0.07$	54.32 ± 3.1	$p = 0.11$	48.13	$p < 0.0001$
	Knockout	8.68		25.68 ± 0.8		43.51 ± 3.1		62.21	

[a] All the experiments were performed on at least three animals for each condition and two to four movies were collected for each animal. The Wilcoxon Mann-Whitney test was used to determine significance for median velocity and median turning angle, and the *t* test was used for average arrest coefficient and confinement index.

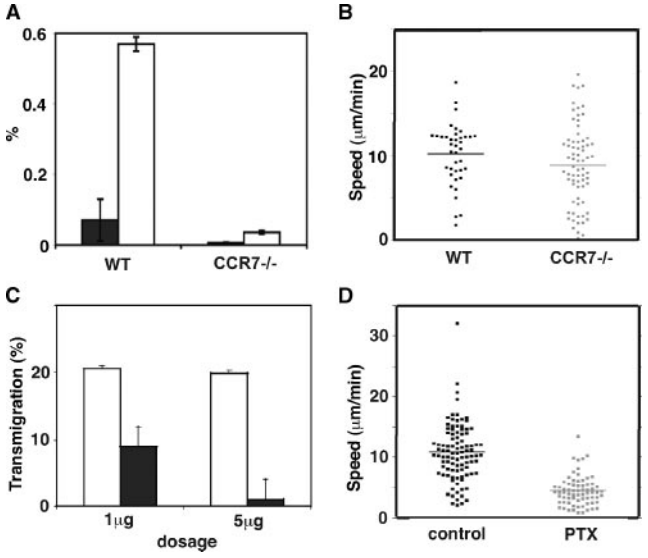

FIGURE 6. $G\alpha_i$ protein-coupled receptors, but not CCR7, are required for normal naive T lymphocyte motility. *A*, Transferred naive $CCR7^{-/-}$ T cells (□) enter the LN with reduced efficiency, a small percentage of central memory T cells (■) were shown. Approximately 5×10^6 purified CFSE-labeled $CD4^+CD62L^+$ T lymphocytes from either $CCR7^{-/-}$ or WT were transferred into WT recipients by tail vein injection. Eighteen hours later, the inguinal LN was harvested and analyzed by flow cytometry. *B*, Representative dot plot of the velocity of $CCR7^{-/-}$ and WT T cells in explanted LNs perfused at 40 μm/s and 20% pO_2. The horizontal bar indicates the median velocity. *C*, WT mice were treated with either 40 (1 μg) or 200 (5 μg) μg/kg of PTX (■), or equal volume of PBS (□). Lymphocyte transmigration was abolished 24 hours after treatment with 5 μg of PTX, and was 50% reduced after treatment with 1 μg of PTX. *D*, T lymphocyte in vivo motility from the LN of mice treated with PBS (control) or 200 μg/kg PTX (PTX), as measured by two-photon imaging. Representative of three experiments.

CD69 on the T cells from the explanted LNs after imaging by flow microfluorometry expression to confirm the CFSE-labeled DO11.10 T cells were activated (data not shown). Activated T lymphocytes moved significantly more slowly (median velocity 4.16 μm/min) compared with naive cells (median velocity 9.16 μm/min) at this time. Differences between their directionality and arrest coefficient were not significant (Table I). When perfusion was maintained at 40 μm/s and pO_2 decreased, the activated cells were able to migrate at their maximum velocity at lower pO_2 than naive T lymphocytes (Fig. 4*B*). Activated T lymphocytes stopped only when pO_2 was <3%, the lowest level that we achieved by bubbling with 100% N_2 in a vessel open to room air. Thus, activated T lymphocytes had lower requirements for pO_2 in the explanted LN compared to naive T lymphocytes.

Chemokines are responsible for the compartmentalization of immune cell within secondary lymphoid tissues with CCR7 playing a major role for T cells (34, 35). CCL21/SLC, the ligands for CCR7, have important roles in T cell entry into (via both high endothelial venules and lymph) and positioning (20, 36), so we transferred CCR7-deficient cells into a WT host, and recorded their locomotion. It must be noted that the entry of CCR7-deficient T cells into LNs after transfer was much less efficient than for WT T cells as previously reported. However, highly pure $CD4^+CD62L^+CD44^-$ naive T cells did enter at levels that allowed tracking, with a small fraction of cells showing central memory T cell phenotype (Fig. 6*A*). We found marginally significant changes in the median velocity (8.68 vs 11.20 μm/min, $p = 0.06$), arrest coefficient (0.18 vs 0.26, $p = 0.07$) and confinement index (0.54 vs 0.44, $p = 0.11$), and with significant increase in median turning angle compared with WT (62.21° vs 48.13°, $p < 0.0001$) (Table I, Fig. 6*B*). Thus, CCR7 contributes a small fraction of signaling for T cell movement within the explanted LNs.

B cell migration in LNs is partially dependent upon $G\alpha_{i2}$ based on genetic experiments (37). We wanted to determine whether there is a general requirement of $G\alpha_i$ activity for T lymphocyte movement in the LN. PTX is internalized by cells and the catalytic subunit enters the cytoplasm and ribosylates $G\alpha_i$, locking coupled GPCR in an inactive state (38–40). Because $G\alpha_i$ is also required for entry into LNs, we took the approach of treating mice with PTX systemically a day after adoptive transfer of CFSE-labeled T lymphocytes, so that the labeled T lymphocytes were already equilibrated in the LN, and then tested T lymphocyte movement 24 h after PTX treatment. To evaluate the appropriate dose we used ex vivo transmigration to CCL21. The doses of PTX that are typically administered as an adjuvant for induction of autoimmune disease or for oral immunization did not inhibit migration of T lymphocytes (Fig. 6*C*). Increasing the dose of PTX 5-fold higher nearly abrogated ex vivo T lymphocyte migration to CCL21 (Fig. 6*C*). Naive T lymphocytes in LN from these high-dose PTX-treated mice were 60% slower than the control (Fig. 6*D*, Table I) ($p < 0.0001$) and had significantly higher arrest coefficients ($p = 0.04$), turning angles ($p < 0.0001$), and confinement indices ($p = 0.01$) compared with the controls (Table I). Thus, $G\alpha_i$ contributed to a large fraction of signaling for rapid naive T lymphocyte migration in LN, but residual, highly confined migration was still detected in the absence of $G\alpha_i$ function. This demonstrates that T cell migration in LNs is mostly directed by GPCR-mediated chemokinetic signals, rather than being an autonomous program.

Thromboxanes act through a GPCR, the thromboxane-prostanoid (TP) receptor (41), and have been implicated in control of T cell-DC interactions via G_0 signaling (42) and immune responses (43). We tested whether TP functions by influencing cell migration in explanted LN by imaging $TP^{-/-}$ T cells transferred into WT mice. We found no difference between $TP^{-/-}$ and control T cells when comparing speed, arrest coefficient, confinement index, and turning angle (Table II). To more generally test the role of arachidonic acid metabolites in T cell migration in the LN, we treated mice with 250 mg/kg cyclooxygenase/lipoxygenase inhibitor

Table II. *Summary table of T lymphocyte motility parameters for experiments determining the importance of TP and G2A, two GPCRs in the arachidonic acid cascade*[a]

Experiment	Cell Type	Speed (μm/min)		Arrest Coefficient (%)		Confinement Index (%)		Turning Angle (°)	
TP	Control	9.71 ± 0.6	$p = 0.95$	20.64 ± 2.1	$p = 0.28$	60.38 ± 5.2	$p = 0.36$	64.23 ± 8.9	$p = 0.62$
	Knockout	9.42 ± 0.3		29.02 ± 5.6		52.82 ± 3.4		73.96 ± 7.4	
G2A	Control	10.11 ± 0.8	$p = 0.88$	21.37 ± 1.2	$p = 0.44$	59.47 ± 2.2	$p = 0.72$	61.34 ± 7.6	$p = 0.92$
	Knockout	9.84 ± 1.1		27.19 ± 7.2		56.4 ± 4.5		62.06 ± 9.5	

[a] These were done using the confocal microscope to collect 2D data sets. All the experiments were performed on at least three animals for each condition and two to four movies were collected for each animal.

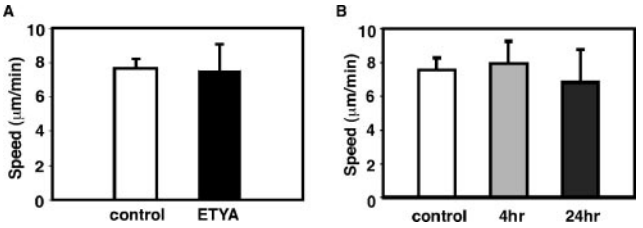

FIGURE 7. Evaluation of two lipid signaling pathways for effect on naive T cell migration. *A*, Blockade of arachidonic acid pathway has no effect on T cell migration speed. Confocal microscopy was used to measure the 2D motility. T cell locomotion speed from mice either vehicle treated (control) or treated with 250 mg/kg ETYA (ETYA) show no significant difference (7.63 vs 7.50 μm/min). *B*, FTY720 treatment does not effect T cell migration speed in LN. T cell migration speed from mice treated with vehicle (control) or FTY720 6 mg/mouse for 4 h (4 h) or 24 h (24 h) show no significant difference when comparing their 2D motility speed (7.59 vs 7.97 vs 6.81 μm/min).

5,8,11,14-eicosatetraynoic acid (ETYA) i.p. (44). Treatment with this concentration of ETYA for 18 h decreased PGE_2 10-fold in LNs (data not shown). We used confocal microscopy to image explanted LNs from mice treated or untreated with ETYA and found no significant difference in the two-dimensional (2D) motility speed (7.63 vs 7.5 μm/min) (Fig. 7*A*). Thus, we found no evidence for a role of arachidonic acid metabolites in control of basal T cell migration in explanted LNs.

Lipid mediators like shpingosine-1-phospate (S1P) and lysophosphatidylcholine acts through GPCR and can mediate chemotaxis of lymphocytes. It has been demonstrated that the $G\alpha_i$ coupled S1P receptor 1 ($S1P_1$) antagonists have no effect on T cell migration in T cell zones (45). We found similar results with the $S1P_1$ down-regulating agonist FTY720 (46). Oral gavage with 6 μg/kg FTY720 had no effect on T cell migration in T cell zones of explanted LN (Fig. 7*B*). The efficacy of FTY720 in this experiment was verified by the dramatic decrease in circulating T cells (data not shown). Lysophosphatidylcholine mediates T cell chemotaxis through G2A, a GPCR that couples to $G\alpha_s$, $G\alpha_{13}$, and $G\alpha_q$ and has diverse biological effects (47–50). However, we found that $G2A^{-/-}$ naive T cells migrated at the same speed as control T cells in explanted LNs (Table II).

In summary, perfusion rate, pO_2, depth, and $G\alpha_i$ were found to be important for controlling T cell migration speed in explanted LN. Necessary pO_2 levels were higher than physiological levels measured in vivo, but were lower than standard perfusion conditions. Ag-activated T cells, in contrast, migrated at physiological pO_2 levels in explanted LNs. We found no essential role of CCR7, TP, arachidonic acid metabolites, $S1P_1$, or G2A for naive T cell migration.

Discussion

We have developed a closed system for imaging an intact LN with controlled temperature, pO_2, and perfusion velocity to determine threshold levels of pO_2 and perfusion velocity that support high T lymphocyte motility. Surprisingly, the pO_2 required to maintain naive T cell mobility was twice the physiological level, as measured in surgically exposed LN in live animals. This higher requirement of pO_2 may reflect limitations in the diffusion of higher m.w. and slower diffusing nutrients like glucose, thus changing the balance of oxidative phosphorylation and glycolysis used to generate ATP, or a higher requirement for O_2-dependent signal generation in the explanted LN. An example of an O_2-dependent signal would be the use of O_2 to generate leukotrienes and PGs, which may have a role in modulating lymphocyte motility. Although we were unable to establish conditions under which naive lymphocytes could migrate with physiological pO_2 in explanted LNs, we were able to obtain high mobility with pO_2 much lower than the routinely used 95%. Although there is no evidence that this high level of pO_2 has caused toxic effects or artifacts, the ability to achieve rapid locomotion at more physiological pO_2 is attractive.

During human T lymphocyte activation, metabolism shifts from a mixture of oxidative phosphorylation and glycolysis, to primarily anaerobic glycolysis (51, 52). Mandeville and Wilkinson (53) have shown that human lymphoblasts migrate under anaerobic conditions in vitro, but ours is the first study to address pO_2 in the context of intact lymphoid tissues and with naive T lymphocytes. Mempel et al. (18) noted that lymphocyte motility stopped immediately when blood flow stopped in intravital experiments and suggested that this could be due to O_2 requirements. However, we would suggest that the rapid decrease in motility is more likely due to loss of perfusion, such that the specific limiting metabolite or signal could not be identified in that study. We found that activated T lymphocytes can migrate under lower pO_2 than naive lymphocytes, which is consistent with these metabolic differences noted above. Naive T lymphocytes recirculate and function almost exclusively in secondary lymphoid tissues, which are well supplied by blood flow. In contrast, activated T lymphocytes must function in diverse peripheral tissue sites, which may include hypoxic regions of tumors or sites of tissue injury that may be hypoxic due to damaged or abnormal vasculature (54). Thus, it is likely to be functionally important that activated T cells can migrate at lower pO_2.

Hypoxia inducible factor controls the expression levels of several essential genes that are required for cell and tissue adaptation to hypoxia including glucose transporters, glycolytic enzymes, vascular endothelial cell growth factor, NO synthase, and erythropoietin (55, 56). T cell activation also up-regulates glucose transporters and glycolytic enzymes (57), perhaps to prepare the cells for entry into hypoxic environments.

We established that the pO_2 in the explanted LN is similar to the pO_2 of the medium at depths of up to 500 μm in contrast to studies of ex vivo skeletal muscle tissue, in which the tissue pO_2 is always lower than the medium pO_2 (27). Diffusion of O_2 across tissues is not simply governed by Fick diffusion laws for a homogeneous material because tissues will have regional difference in diffusion based on different capsule composition and integrity (58), the volume fraction of cells and the tortuosity factor established by barriers to diffusion in the intercellular spaces of the tissue (59). Thus, it is possible that LNs have higher O_2 permeability than muscle tissue, but its more likely that higher consumption of O_2 in muscle (27) compared with LNs may be responsible for the difference in apparent O_2 penetration. Although lymphocytes move rapidly in LNs, this amoeboid movement generates very little contractile force (53) and may require relatively little ATP compared with muscle contraction. LNs also have an elaborate conduit system that may allow perfusion of the LN interior by medium that is flowing over the LN surface (60).

To further understand the mechanism behind hypoxia induced stopping, we tested the hypothesis that hypoxia hampered lymphocyte migration through the adenosine receptor $A_{2A}R$. Could modulating $A_{2A}R$ pathway, using antagonist to $A_{2A}R$, lead to sustained motility under hypoxic conditions? To test this, we used a potent antagonist ZM241385 for $A_{2A}R$ and also $A_{2A}R^{-/-}$ mice. These mice develop extensive tissue damage in response to concentrations of inflammatory stimuli that would

not elicit responses in WT mice (61). In a lung injury model, oxygenation weakened the $A_{2A}R$-mediated anti-inflammatory mechanism that was driven by hypoxia, and exacerbates lung injury (62). However, in $A_{2A}R^{-/-}$ T cells and T cells treated with antagonists stopped migrating at the same pO_2 as control cells. Therefore, the anti-inflammatory action of $A_{2A}R$ does not involve modulation of naive T cell migration.

We found that naive T lymphocyte locomotion in explanted LNs requires a critical threshold perfusion velocity (Fig. 3). Delivery of O_2 is likely one function of perfusion, but the permeability factors in tissues for larger metabolites like glucose and lactic acid are 10- to 100-fold lower than for O_2 (63). Thus, it is likely that the perfusion velocity threshold is set by the need to maintain steep diffusion gradients for glucose into the LN and waste products of anaerobic metabolism like lactic acid out of the LN. Alternatively, perfusion above a certain threshold may be required to drive media through the reticular fiber network as suggested above, serendipitously generating a circulatory system for the explanted LN. Thus, the internal perfusion of explanted LNs may be even more extensive than in vivo by capillaries.

We found the naive cells moved slower in the superficial areas of the LN compared with the deep paracortex. The higher confinement suggests that the architecture of the subcapsular area may contain more obstacles that must be negotiated by migrating T lymphocytes. A recent article suggested that the fibroblastic reticular cell network regulates lymphocyte migration, by shaping the microanatomy within the LN (16). Because pO_2 is constant throughout this depth range and metabolite diffusion would seem to favor faster movement near the capsule, it is most likely that the difference is due to tissue architecture. For example, DC organization and dynamics are very different in the subcapsular, interfollicular and paracortical areas of the LN (8). Because DCs are a major interaction partner for T lymphocytes, it is likely that these differences would result in differences in movement characteristic unless there were compensating factors. Intravital microscopy studies noted a similar difference in shallow and deep movement in the popliteal LN (18), but not the inguinal LN (14). These differences could be due to specific differences in proximity to blood vessels and the specific architecture of the fixed views of the popliteal and inguinal LNs as presented in intravital microscopy. It is not known whether there is any functional significance to these differences in motility in different compartments.

We found that naive $CCR7^{-/-}$ T cells were able to inefficiently traffic to the LN. It has been shown that central memory T cells can use CXCR4 to enter LN via high endothelial venules. We rigorously depleted memory cells from the transferred populations such that we are confident that the tracked cells displaying essentially normal migration velocity were $CCR7^{-/-}$ naive T cells. We were surprised that in our hands, $CCR7^{-/-}$ naive T cells migrated relatively normally in light of recent in vitro studies with DCs, suggesting the CCL21 is a major chemokinetic factor for naive T cells (64). A recent publication by Okada et al. (65) found similar results that PTX reduces T lymphocyte motility and increases the turning angle of naive T lymphocytes when used to treat T cells just before transfer into mice. Thus, two approaches to pertussis toxin treatment lead to similar results. We also concur with both Okada et al. (65) and Worbs et al. (32) that $CCR7^{-/-}$ T cells display a small decrease in motility in the LN. Thus, CCR7 contributes only a small fraction of the $G\alpha_i$-dependent naive T cell mobility in the LN. Worbs et al. (32) also reported slower movement in the subcapsular zone compared with the deep paracortex, in agreement with our findings.

Treating the mice with high doses of PTX resulted in decreased T cell locomotion speed and increased confinement of T cells in explanted LNs. Chemokine receptors, TP, $S1P_1$, and other receptors such as ORG1, DOR1 signal through $G\alpha_i$, and they are expressed on T cells. These receptors regulate a range of functions including chemotaxis (66), differentiation (67), proliferation, and cytokine production (68). In a recent report, lymphocytes treated with PTX exhibited only a partial reduction in LN egress, though a total block in LN entry (69). Together with our results, we conclude that $G\alpha_i$-coupled receptors largely determine lymphocyte motility within LNs. The confined $G\alpha_i$-independent movement may be mediated by GPCR that use other G-proteins. For example, TP couples to $G\alpha_q$, $G\alpha_{i2}$, $G\alpha_{11/12/13/16}$ (70) and has been shown to regulate naive T lymphocyte migration (42). However, we examined $TP^{-/-}$ T cells and the situation in which ETYA was used to inhibit PG, thromboxane, and lipoxygenase production and found no decrease in naive T cell migration. The failure to detect significant changes in migration with any single receptor system may indicate either that these systems are not involved in stimulation of naive T cell migration or that there are redundant mechanisms such that elimination of any one of these receptor systems is without effect. Cahalan and colleagues (15) have argued that naive T cell migration appears to be autonomous. Although this statement can be interpreted in different ways, we feel that naive T cell migration is not autonomous in the manner of in vitro migration of cytokine-stimulated T cells, which migrate autonomously when they have an appropriate substrate like ICAM-1 (71). We cannot rule out that the residual migration detected in the presence of PTX may be a more strictly autonomous program mediated by other hormone or cytokine receptors, including receptor tyrosine kinases (72) and receptors for the JAK-STAT pathways (73).

Acknowledgments

We thank Dr. Wenbiao Gan for setting up the microscope, Dr. Thomas O. Cameron and Teresa Wu for assisting early anoxic experiments, Drs. Rod Braun and Jennifer Lanzen for assisting the in vivo LN pO_2 measurement, Dr. Thomas O. Cameron, V. Kaye Thomas, and Dr. J. C. Rathmell for critical reading of the manuscript, and members of the Dustin laboratory for thoughtful discussions.

Disclosures

The authors have no financial conflict of interest.

References

1. Hedrick, S. M., E. A. Nielsen, J. Kavaler, D. I. Cohen, and M. M. Davis. 1984. Sequence relationships between putative T-cell receptor polypeptides and immunoglobulins. *Nature* 308: 153–158.
2. Babbitt, B. P., P. M. Allen, G. Matsueda, E. Haber, and E. R. Unanue. 1985. Binding of immunogenic peptides to Ia histocompatibility molecules. *Nature* 317: 359–361.
3. Ingulli, E., A. Mondino, A. Khoruts, and M. K. Jenkins. 1997. In vivo detection of dendritic cell antigen presentation to $CD4^+$ T cells. *J. Exp. Med.* 185: 2133–2141.
4. Turley, S. J., K. Inaba, W. S. Garrett, M. Ebersold, J. Unternaehrer, R. M. Steinman, and I. Mellman. 2000. Transport of peptide-MHC class II complexes in developing dendritic cells. *Science* 288: 522–527.
5. Balazs, M., F. Martin, T. Zhou, and J. Kearney. 2002. Blood dendritic cells interact with splenic marginal zone B cells to initiate T-independent immune responses. *Immunity* 17: 341–352.
6. Randolph, G. J., S. Beaulieu, M. Pope, I. Sugawara, L. Hoffman, R. M. Steinman, and W. A. Muller. 1998. A physiologic function for *p*-glycoprotein (MDR-1) during the migration of dendritic cells from skin via afferent lymphatic vessels. *Proc. Natl. Acad. Sci. USA* 95: 6924–6929.
7. Muraille, E., R. Giannino, P. Guirnalda, I. Leiner, S. Jung, E. G. Pamer, and G. Lauvau. 2005. Distinct in vivo dendritic cell activation by live versus killed *Listeria monocytogenes*. *Eur. J. Immunol.* 35: 1463–1471.

8. Lindquist, R. L., G. Shakhar, D. Dudziak, H. Wardemann, T. Eisenreich, M. L. Dustin, and M. C. Nussenzweig. 2004. Visualizing dendritic cell networks in vivo. *Nat. Immunol.* 5: 1243–1250.
9. Marchesi, V. T., and J. L. Gowans. 1964. The migration of lymphocytes through the endothelium of venules in lymph nodes: an electron microscope study. *Proc. R Soc. Lond. B Biol. Sci.* 159: 283–290.
10. Gowans, J. L., and E. J. Knight. 1964. The route of re-circulation of lymphocytes in the rat. *Proc. R Soc. Lond. B Biol. Sci.* 159: 257–282.
11. von Andrian, U. H., and C. R. Mackay. 2000. T-cell function and migration: two sides of the same coin. *N. Engl. J. Med.* 343: 1020–1034.
12. Denk, W., J. H. Strickler, and W. W. Webb. 1990. Two-photon laser scanning fluorescence microscopy. *Science* 248: 73–76.
13. Miller, M. J., S. H. Wei, I. Parker, and M. D. Cahalan. 2002. Two-photon imaging of lymphocyte motility and antigen response in intact lymph node. *Science* 296: 1869–1873.
14. Shakhar, G., R. L. Lindquist, D. Skokos, D. Dudziak, J. H. Huang, M. C. Nussenzweig, and M. L. Dustin. 2005. Stable T cell-dendritic cell interactions precede the development of both tolerance and immunity in vivo. *Nat. Immunol.* 6: 707–714.
15. Miller, M. J., S. H. Wei, M. D. Cahalan, and I. Parker. 2003. Autonomous T cell trafficking examined in vivo with intravital two-photon microscopy. *Proc. Natl. Acad. Sci. USA* 100: 2604–2609.
16. Bajenoff, M., J. G. Egen, L.Y. Koo, J. P. Laugier, F. Brau, N. Glaichenhaus, and R. N. Germain. 2006. Stromal cell networks regulate lymphocyte entry, migration, and territoriality in lymph nodes. *Immunity* 6: 989–1001.
17. Caldwell, C. C., H. Kojima, D. Lukashev, J. Armstrong, M. Farber, S. G. Apasov, and M. V. Sitkovsky. 2001. Differential effects of physiologically relevant hypoxic conditions on T lymphocyte development and effector functions. *J. Immunol.* 167: 6140–6149.
18. Mempel, T. R., S. E. Henrickson, and U. H. Von Andrian. 2004. T-cell priming by dendritic cells in lymph nodes occurs in three distinct phases. *Nature* 427: 154–159.
19. Forster, R., A. Schubel, D. Breitfeld, E. Kremmer, I. Renner-Muller, E. Wolf, and M. Lipp. 1999. CCR7 coordinates the primary immune response by establishing functional microenvironments in secondary lymphoid organs. *Cell* 99: 23–33.
20. Bromley, S. K., S. Y. Thomas, and A. D. Luster. 2005. Chemokine receptor CCR7 guides T cell exit from peripheral tissues and entry into afferent lymphatics. *Nat. Immunol.* 6: 895–901.
21. Debes, G. F., C. N. Arnold, A. J. Young, S. Krautwald, M. Lipp, J. B. Hay, and E. C. Butcher. 2005. Chemokine receptor CCR7 required for T lymphocyte exit from peripheral tissues. *Nat. Immunol.* 6: 889–894.
22. Chen, J. F., Z. Huang, J. Ma, J. Zhu, R. Moratalla, D. Standaert, M. A. Moskowitz, J. S. Fink, and M. A. Schwarzschild. 1999. A_{2A} adenosine receptor deficiency attenuates brain injury induced by transient focal ischemia in mice. *J. Neurosci.* 19: 9192–9200.
23. Braun, R. D., J. L. Lanzen, S. A. Snyder, and M. W. Dewhirst. 2001. Comparison of tumor and normal tissue oxygen tension measurements using OxyLite or microelectrodes in rodents. *Am. J. Physiol.* 280: H2533–H2544.
24. Denk, W., K. R. Delaney, A. Gelperin, D. Kleinfeld, B. W. Strowbridge, D. W. Tank, and R. Yuste. 1994. Anatomical and functional imaging of neurons using 2-photon laser scanning micros. *J. Neurosci. Methods* 54: 151–162.
25. Grutzendler, J., N. Kasthuri, and W. B. Gan. 2002. Long-term dendritic spine stability in the adult cortex. *Nature* 420: 812–816.
26. Majewska, A., G. Yiu, and R. Yuste. 2000. A custom-made two-photon microscope and deconvolution system. *Pflugers Arch.* 441: 398–408.
27. Eu, J. P., J. M. Hare, D. T. Hess, M. Skaf, J. Sun, I. Cardenas-Navina, Q. A. Sun, M. Dewhirst, G. Meissner, and J. S. Stamler. 2003. Concerted regulation of skeletal muscle contractility by oxygen tension and endogenous nitric oxide. *Proc. Natl. Acad. Sci. USA* 100: 15229–15234.
28. von Andrian, U. H. 1996. Intravital microscopy of the peripheral lymph node microcirculation in mice. *Microcirculation* 3: 287–300.
29. Bousso, P., and E. A. Robey. 2004. Dynamic behavior of T cells and thymocytes in lymphoid organs as revealed by two-photon microscopy. *Immunity* 21: 349–355.
30. Sitkovsky, M. V., D. Lukashev, S. Apasov, H. Kojima, M. Koshiba, C. Caldwell, A. Ohta, and M. Thiel. 2004. Physiological control of immune response and inflammatory tissue damage by hypoxia-inducible factors and adenosine A2A receptors. *Annu. Rev. Immunol.* 22: 657–682.
31. Gretz, J. E., A. O. Anderson, and S. Shaw. 1997. Cords, channels, corridors and conduits: critical architectural elements facilitating cell interactions in the lymph node cortex. *Immunol. Rev.* 156: 11–24.
32. Worbs, T., T. R. Mempel, J. Bolter, U. H. von Andrian, and R. Forster. 2007. CCR7 ligands stimulate the intranodal motility of T lymphocytes in vivo. *J. Exp. Med.* 204: 489–495.
33. Miller, M. J., A. S. Hejazi, S. H. Wei, M. D. Cahalan, and I. Parker. 2004. T cell repertoire scanning is promoted by dynamic dendritic cell behavior and random T cell motility in the lymph node. *Proc. Natl. Acad. Sci. USA* 101: 998–1003.
34. Campbell, D. J., C. H. Kim, and E. C. Butcher. 2003. Chemokines in the systemic organization of immunity. *Immunol. Rev.* 195: 58–71.
35. Muller, G., U. E. Hopken, H. Stein, and M. Lipp. 2002. Systemic immunoregulatory and pathogenic functions of homeostatic chemokine receptors. *J. Leukocyte Biol.* 72: 1–8.
36. Stein, J. V., A. Rot, Y. Luo, M. Narasimhaswamy, H. Nakano, M. D. Gunn, A. Matsuzawa, E. J. Quackenbush, M. E. Dorf, and U. H. von Andrian. 2000. The CC chemokine thymus-derived chemotactic agent 4 (TCA-4, secondary lymphoid tissue chemokine, 6Ckine, exodus-2) triggers lymphocyte function-associated antigen 1-mediated arrest of rolling T lymphocytes in peripheral lymph node high endothelial venules. *J. Exp. Med.* 191: 61–76.
37. Han, S. B., C. Moratz, N. N. Huang, B. Kelsall, H. Cho, C. S. Shi, O. Schwartz, and J. H. Kehrl. 2005. Rgs1 and Gnai2 regulate the entrance of B lymphocytes into lymph nodes and B cell motility within lymph node follicles. *Immunity* 22: 343–354.
38. Bokoch, G. M., T. Katada, J. K. Northup, E. L. Hewlett, and A. G. Gilman. 1983. Identification of the predominant substrate for ADP-ribosylation by islet activating protein. *J. Biol. Chem.* 258: 2072–2075.
39. Jacquemin, C., H. Thibout, B. Lambert, and C. Correze. 1986. Endogenous ADP-ribosylation of Gs subunit and autonomous regulation of adenylate cyclase. *Nature* 323: 182–184.
40. Kaslow, H. R., and D. L. Burns. 1992. Pertussis toxin and target eukaryotic cells: binding, entry, and activation. *FASEB J.* 6: 2684–2690.
41. Hirata, M., Y. Hayashi, F. Ushikubi, Y. Yokota, R. Kageyama, S. Nakanishi, and S. Narumiya. 1991. Cloning and expression of cDNA for a human thromboxane A2 receptor. *Nature* 349: 617–620.
42. Kabashima, K., T. Murata, H. Tanaka, T. Matsuoka, D. Sakata, N. Yoshida, K. Katagiri, T. Kinashi, T. Tanaka, M. Miyasaka, et al. 2003. Thromboxane A2 modulates interaction of dendritic cells and T cells and regulates acquired immunity. *Nat. Immunol.* 4: 694–701.
43. Thomas, D. W., P. N. Rocha, C. Nataraj, L. A. Robinson, R. F. Spurney, B. H. Koller, and T. M. Coffman. 2003. Proinflammatory actions of thromboxane receptors to enhance cellular immune responses. *J. Immunol.* 171: 6389–6395.
44. Taylor, A. S., A. R. Morrison, and J. H. Russell. 1985. Incorporation of 5,8,11,14-eicosatetraynoic acid (ETYA) into cell lipids: competition with arachidonic acid for esterification. *Prostaglandins* 29: 449–458.
45. Wei, S. H., H. Rosen, M. P. Matheu, M. G. Sanna, S. K. Wang, E. Jo, C. H. Wong, I. Parker, and M. D. Cahalan. 2005. Sphingosine 1-phosphate type 1 receptor agonism inhibits transendothelial migration of medullary T cells to lymphatic sinuses. *Nat. Immunol.* 6: 1228–1235.
46. Chiba, K., Y. Yanagawa, Y. Masubuchi, H. Kataoka, T. Kawaguchi, M. Ohtsuki, and Y. Hoshino. 1998. FTY720, a novel immunosuppressant, induces sequestration of circulating mature lymphocytes by acceleration of lymphocyte homing in rats. I. FTY720 selectively decreases the number of circulating mature lymphocytes by acceleration of lymphocyte homing. *J. Immunol.* 160: 5037–5044.
47. Radu, C. G., L. V. Yang, M. Riedinger, M. Au, and O. N. Witte. 2004. T cell chemotaxis to lysophosphatidylcholine through the G2A receptor. *Proc. Natl. Acad. Sci. USA* 101: 245–250.
48. Lin, P., and R. D. Ye. 2003. The lysophospholipid receptor G2A activates a specific combination of G proteins and promotes apoptosis. *J. Biol. Chem.* 278: 14379–14386.
49. Weng, Z., A. C. Fluckiger, S. Nisitani, M. I. Wahl, L. Q. Le, C. A. Hunter, A. A. Fernal, M. M. Le Beau, and O. N. Witte. 1998. A DNA damage and stress inducible G protein-coupled receptor blocks cells in G_2-M. *Proc. Natl. Acad. Sci. USA* 95: 12334–12339.
50. Yang, L. V., C. G. Radu, L. Wang, M. Riedinger, and O. N. Witte. 2005. G_i-independent macrophage chemotaxis to lysophosphatidylcholine via the immunoregulatory GPCR G2A. *Blood* 105: 1127–1134.
51. Bental, M., and C. Deutsch. 1993. Metabolic changes in activated T cells: an NMR study of human peripheral blood lymphocytes. *Magn. Reson. Med.* 29: 317–326.
52. Rathmell, J. C., E. A. Farkash, W. Gao, and C. B. Thompson. 2001. IL-7 enhances the survival and maintains the size of naive T cells. *J. Immunol.* 167: 6869–6876.
53. Mandeville, R. P., and P. C. Wilkinson. 1982. Locomotion of human lymphoblasts towards glucose and other sugars: effects of pH, temperature and oxygen. *Clin. Exp. Immunol.* 50: 479–486.
54. Iparraguirre, A., and W. Weninger. 2003. Visualizing T cell migration in vivo. *Int. Arch. Allergy Immunol.* 132: 277–293.
55. Nakamura, H., Y. Makino, K. Okamoto, L. Poellinger, K. Ohnuma, C. Morimoto, and H. Tanaka. 2005. TCR engagement increases hypoxia-inducible factor-1α protein synthesis via rapamycin-sensitive pathway under hypoxic conditions in human peripheral T cells. *J. Immunol.* 174: 7592–7599.
56. Iyer, N. V., L. E. Kotch, F. Agani, S. W. Leung, E. Laughner, R. H. Wenger, M. Gassmann, J. D. Gearhart, A. M. Lawler, A. Y. Yu, and G. L. Semenza. 1998. Cellular and developmental control of O_2 homeostasis by hypoxia-inducible factor 1α. *Genes Dev.* 12: 149–162.
57. Jacobs, S. R., and J. C. Rathmell. 2005. Lymphocyte selection by starvation: glucose metabolism and cell death. *Trends Immunol.* 27: 4–7.
58. Sniekers, Y. H., and C. C. van Donkelaar. 2005. Determining diffusion coefficients in inhomogeneous tissues using fluorescence recovery after photobleaching. *Biophys. J.* 89: 1302–1307.
59. Lipinski, H. G. 1989. Model calculations of oxygen supply to tissue slice preparations. *Phys. Med. Biol.* 34: 1103–1111.
60. Ebnet, K., E. P. Kaldjian, A. O. Anderson, and S. Shaw. 1996. Orchestrated information transfer underlying leukocyte endothelial interactions. *Annu. Rev. Immunol.* 14: 155–177.

61. Ohta, A., and M. Sitkovsky. 2001. Role of G-protein-coupled adenosine receptors in downregulation of inflammation and protection from tissue damage. *Nature* 414: 916–920.
62. Thiel, M., A. Chouker, A. Ohta, E. Jackson, C. Caldwell, P. Smith, D. Lukashev, I. Bittmann, and M. V. Sitkovsky. 2005. Oxygenation inhibits the physiological tissue-protecting mechanism and thereby exacerbates acute inflammatory lung injury. *PLoS Biol.* 3: e174.
63. Akeson, M. A., and D. N. Munns. 1989. Lipid bilayer permeation by neutral aluminum citrate and by three α-hydroxy carboxylic acids. *Biochim. Biophys. Acta* 984: 200–206.
64. Stachowiak, A. N., Y. Wang, Y. C. Huang, and D. J. Irvine. 2006. Homeostatic lymphoid chemokines synergize with adhesion ligands to trigger T and B lymphocyte chemokinesis. *J. Immunol.* 177: 2340–2348.
65. Okada, T., and J. G. Cyster. 2007. CC chemokine receptor 7 contributes to G_i-dependent T cell motility in the lymph node. *J. Immunol.* 178: 2973–2978.
66. Ebert, L. M., P. Schaerli, and B. Moser. 2005. Chemokine-mediated control of T cell traffic in lymphoid and peripheral tissues. *Mol. Immunol.* 42: 799–809.
67. Luther, S. A., and J. G. Cyster. 2001. Chemokines as regulators of T cell differentiation. *Nat. Immunol.* 2: 102–107.
68. Bacon, K. B., B. A. Premack, P. Gardner, and T. J. Schall. 1995. Activation of dual T cell signaling pathways by the chemokine RANTES. *Science* 269: 1727–1730.
69. Lo, C. G., Y. Xu, R. L. Proia, and J. G. Cyster. 2005. Cyclical modulation of sphingosine-1-phosphate receptor 1 surface expression during lymphocyte recirculation and relationship to lymphoid organ transit. *J. Exp. Med.* 201: 291–301.
70. Parent, J. L., P. Labrecque, M. J. Orsini, and J. L. Benovic. 1999. Internalization of the TXA2 receptor α and β isoforms. Role of the differentially spliced COOH terminus in agonist-promoted receptor internalization. *J. Biol. Chem.* 274: 8941–8948.
71. Dustin, M. L., S. K. Bromley, Z. Kan, D. A. Peterson, and E. R. Unanue. 1997. Antigen receptor engagement delivers a stop signal to migrating T lymphocytes. *Proc. Natl. Acad. Sci. USA* 94: 3909–3913.
72. Wu, J., and H. Luo. 2005. Recent advances on T-cell regulation by receptor tyrosine kinases. *Curr. Opin. Hematol.* 12: 292–297.
73. Weissenbach, M., T. Clahsen, C. Weber, D. Spitzer, D. Wirth, D. Vestweber, P. C. Heinrich, and F. Schaper. 2004. Interleukin-6 is a direct mediator of T cell migration. *Eur. J. Immunol.* 34: 2895–2906.